Interaction between Poly(9,9-bis(6′-*N*,*N*,*N*-trimethylammonium)hexyl)fluorene phenylene) Bromide and DNA as Seen by Spectroscopy, Viscosity, and Conductivity: Effect of Molecular Weights and DNA Secondary Structure

María Monteserín,[†] Hugh D. Burrows,*[,‡] Artur J. M. Valente,[‡] Ricardo Mallavia,[§] Roberto E. Di Paolo,[||] Antonio L. Maçanita,[||] and María J. Tapia*[,†]

Departamento de Química, Universidad de Burgos, Plaza Misael Bañuelos, Burgos 09001, Spain, Departamento de Química, Universidade de Coimbra, 3004-535 Coimbra, Portugal, Instituto de Biología Molecular y Celular, Universidad Miguel Hernández, Elche 03202, Alicante, Spain, and Departamento de Engenharia Química e Biologica, Instituto Superior Técnico (IST), Avenida Rovisco Pais, P1049-001, Lisboa, Portugal

Received: July 18, 2008; Revised Manuscript Received: October 18, 2008

The interaction between three poly(9,9-bis(6-*N*,*N*,*N*-trimethylammonium)hexyl)fluorene phenylene) bromide (HTMA-PFP) samples of different molecular weights ($\overline{M_n}$ = 14.5, 30.1 and 61.3 kg/mol) and both dsDNA and ssDNA secondary structures has been studied using UV−visible absorption and fluorescence spectroscopies (including steady-state, time-resolved, and anisotropy measurements for the latter), viscosity, and electrical conductivity in 4% (v/v) DMSO−water mixtures. At low nucleic acid concentrations, formation of a 1:1 complex in terms of HTMA-PFP repeat units and DNA bases occurs. This interaction results in quenching of polymer emission. For higher molar ratios of DNA to HTMA-PFP, corresponding to charge neutralization, a second process is observed that is attributed to aggregate formation. From the changes in the absorption spectra, the polymer aggregation constant and the aggregate absorption spectra were calculated by applying an iterative method. Polymer aggregation dramatically quenches HTMA-PFP fluorescence in the region of the electroneutrality point. Under these conditions, the ratio of the emission intensity at 412 nm (maximum) to that at 434 nm (I^{412}/I^{434}) reaches a minimum, the electrical conductivity decreases, and the viscosity of the solution remains constant, showing that the DNA concentration can be determined through various HTMA-PFP physicochemical properties. With respect to the photophysical parameters (emission quantum yield, shape and shift of emission spectra), no significant differences were observed between dsDNA and ssDNA or with conjugated polymer or DNA molecular weight. The two short-lived components in the fluorescence decays are attributed to the presence of aggregates. Aggregates are also suggested to be responsible for the decrease in the fluorescence anisotropy through interchain exciton migration.

Introduction

Conjugated polyelectrolytes (CPEs) are π-conjugated polymers with side chains containing charged groups,[1] which are finding applications in both chemical and biological sensing and in various optoelectronic devices. However, their solubility in water is normally limited because of the hydrophobicity of the conjugated backbones and to $\pi-\pi$ interactions between adjacent polymer chains, leading to aggregation to form ill-defined clusters.[2] This trend to aggregation leads to low photoluminescence quantum efficiencies and limits their applications in light-emitting diode (LED) displays[3] and biosensors[4] and is particularly evident when the polymer charge is neutralized by interaction with oppositely charged compounds.[5] This could be an important factor when CPEs are used as DNA sensors.

Cationic conjugated polymers (CCPs) are widely used as DNA biosensors because of the electrostatic interaction with the oppositely charged phosphate groups of the target polynucleotide.[4c] Cationic poly(*para*-phenylenevinylene),[4c] polythiophene derivatives[6] or poly(fluorene-*co*-phenylene) derivatives[7] are widely used. The latter compounds have become particularly popular because they show a relatively high emission quantum yield in aqueous solution, together with blue light emission, and their structures can be easily modified through substitution at the fluorene C9 position.[8]

Various schemes have been developed, largely by Bazan et al., to detect DNA using cationic poly(fluorene-*co*-phenylene)s as biosensors. Many of them are based on Förster resonant energy transfer (FRET). In some cases, peptide nucleic acid (PNA) recognition is used. PNAs consist of a polyamide moiety composed of *N*-(2-aminoethyl)glycine and DNA nucleobases attached through methylene carbonyl linkers.[7a] The replacement of the negatively charged sugar−phosphate groups by the polyamide has been used to explain the fact that DNA tends to bind to a PNA chain more tightly than to another DNA chain through Watson−Crick base pairing.[7a] The detection scheme consists of a CCP donor and a dye-labeled PNA acceptor (PNA-C*) with the CCP binding to DNA through electrostatic attraction. If the DNA target is complementary to the PNA-C* probe, FRET is produced because donor (CCP) and acceptor (C*) are within the Förster radius; however, if the PNA is not complementary to the DNA, no energy transfer from CCP to

* Corresponding authors. E-mail: mjtapia@ubu.es (M.J.T.), burrows@ci.uc.pt (H.D.B.). Phone: +34 947258061(M.J.T.), +351 239854482(H.D.B.). Fax: (+34) 947 28831 (M.J.T.), (+351) 239 827703 (H.D.B.).
[†] Universidad de Burgos.
[‡] Universidade de Coimbra.
[§] Universidad Miguel Hernández.
[||] Instituto Superior Técnico (IST).

10.1021/jp806353y CCC: $40.75
Published on Web 01/13/2009

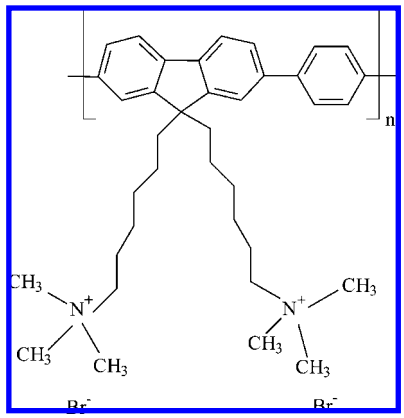

Figure 1. HTMA-PFP chemical structure.

C* is produced.[7a] This scheme allows for specific, direct detection of double-stranded DNA (dsDNA).[7a]

A variation of this scheme, but adding an S1 nuclease enzyme, has been used to detect a mutation in a region of a gene implicated in neurodegenerative dementia by choosing the appropriate PNA probe and using poly(9,9-bis(6′-*N*,*N*,*N*-trimethylammonium)hexyl)fluorene phenylene) iodide as the CCP. Only DNA that matches perfectly with the PNA leads to FRET, whereas other mutant sequences are digested by the enzyme, thereby preventing the energy-transfer process.[8,9] FRET directly from the CCP to a dye-labeled DNA has also been used, without any PNA involved.[10]

Another variant of the FRET process has been developed to determine DNA concentrations using the cationic water-soluble species poly(9,9-bis(6′-*N*,*N*,*N*-trimethylammonium)hexyl)fluorene-*co*-*alt*-1,4-phenylene) bromide, which contains partial substitution of the fluorene units with 2,1,3-benzothiadiazole (PFPB) fragments.[7e] In dilute conditions, the emission of PFPB with 5% 2,1,3-benzothiadiazole (BT) is in the blue region (390−500 nm). However, at higher polymer concentrations, when the polymer is aggregated, energy transfer from the fluorene phenylene repeat units (RUs) to BT is observed, leading to its characteristic green emission (500−700 nm). A similar phenomenon is produced when DNA is added, and DNA-induced aggregation also provokes an increase of the green emission at the expense of the blue. From the intensity ratio between the green and blue emissions upon DNA addition, the DNA concentration can be determined using the appropriate calibration curve.[7e] A similar methodology has been developed with polymers that are structurally close to PFPB to determine dsDNA concentrations in the range from 3×10^{-12} to 2×10^{-5} M.[11]

One of the most widely used polymers for these DNA-sensing experiments is poly(9,9-bis(6′-*N*,*N*,*N*-trimethylammonium)hexyl)-fluorene phenylene) bromide (HTMA-PFP, Figure 1) or the corresponding iodide salt.[7a,f,h,8,12] It is well-known that the iodide derivative of HTMA-PFP forms very tight aggregates in pure water, with chains coming together and forming an inner cylindrical core,[13] and as previously mentioned, complexation with oppositely charge polyelectrolytes (e.g., DNA) brings together PFPB polymer segments (such as in HTMA-PFP), leading to a reduction in the CPE fluorescence. However, the attraction between oppositely charged polymers decreases when a buffer containing 10 mM sodium citrate and 100 mM NaCl is used.[7f]

In this work, we studied the interaction between HTMA-PFP samples with three different molecular weights ($\overline{M_n}$ = 14.5, 30.1 and 61.3 kg/mol) and both salmon testes (2000 bp) dsDNA and thermally denatured single-stranded DNA (ssDNA) in aqueous solution to analyze the effect of polymer molecular weight and DNA secondary structure on the HTMA-PFP/DNA interaction. Moreover, the effect of DNA molecular weight was studied by carrying out experiments with human placenta dsDNA [hereafter dsDNA(HP), 22 kbp]. Although many of the studies reported to date have used oligonucleotides or relatively low-molecular-weight nucleic acids,[14] for many applications, it is important to know what happens with the relatively high-molecular-weight DNA systems reported here. In addition to applying conventional spectroscopic techniques (absorption, steady-state and time-resolved fluorescence, and fluorescence anisotropy), we also used electrical specific conductance, which reports on changes in the structure of ionic solutions, and viscosity, which reflects the size and shape of aggregates formed during HTMA-PFP/DNA complexation. We characterized the aggregation process spectroscopically and show that the DNA molar concentration can be estimated from the changes in the physical properties of the polymer (absorption, emission, electrical conductivity, viscosity) in aqueous solution in a very simple way without the need for a second chromophore attached to either the DNA or the PNA in the more complex FRET process.

Experimental Section

Reagent and Solution Preparation. Three batches of the neutral polymer poly(9,9-bis(6′-bromohexyl)fluorene-1,4-phenylene) were synthesized via Suzuki coupling reaction using 1,4-phenyldiboronic acid and 2,7-dibromo-9,9-bis(6′-bromohexyl)fluorene.[15] For the lowest-molecular-weight batch of polymer, the Suzuki coupling reaction was carried out over 3 days. For the other two batches, the reaction was carried out using different palladium catalysts[16] and was stopped after 12 h. The molecular weights of the three batches of the neutral polymer were characterized by size-exclusion chromatography (SEC) in tetrahydrofuran (THF) as the solvent using polystyrene standards for calibration. For the batch with the highest-molecular-weight polymer, a bimodal distribution was obtained that corresponded to 90.7% of the main distribution (n = 143) and 9.3% of the secondary distribution (n = 36). The other two batches (n = 37 and n = 64) showed regular average molecular weight distributions.

The cationic conjugated polyeletrolyte poly(9,9-bis(6′-*N*,*N*,*N*-trimethylammonium)hexyl)fluorene phenylene) bromide (HTMA-PFP, Figure 1) was obtained by treating the neutral poly(9,9-bis(6′-bromohexyl)fluorene phenylene) with trimethylamine gas following the procedure described elsewhere.[17] We assume, in agreement with previous reports,[18] that almost quantitative conversion of the neutral copolymer into the cationic one (HTMA-PFP) occurred, and that did not affect the degree of polymerization.

According to this assumption, the number-average molecular weight ($\overline{M_n}$) values of the three batches of HTMA-PFP were 14.5, 30.1, and 61.3 kg/mol (where the last polymer exhibited a bimodal distribution with the highest fraction at $\overline{M_n}$ = 71.1 kg/mol and the lowest at $\overline{M_n}$ = 16.6 kg/mol).

HTMA-PFP has a low solubility in water, but can be dissolved in dimethyl sulfoxide−water mixtures. Stock polymer solutions with concentrations of around 9.6×10^{-2} g/L (1.38×10^{-4} mol/L in repeat units) were prepared in dimethyl sulfoxide (DMSO, Aldrich, spectrophotometric grade) and were kept under continuous stirring overnight. Aliquots of this solution were diluted with Millipore-Q water to give solutions with polymer concentrations of $(3.0-5.5) \times 10^{-6}$ M in terms

of repeat units [(2.1−3.8) × 10^{-3} g/L] in 4% (v/v) DMSO−water mixtures that were used for the measurements.

Solutions of DNA solutions of salmon testes (dsDNA, approximately 2000 bp) and human placenta [dsDNA(HP), about 22 kbp] from Sigma were prepared in Millipore-Q water. For the spectroscopic experiments, stock solutions had a concentration of around 0.15 mg/mL (4.5 × 10^{-4} M, ε_{260} = 6600 mol^{-1} L cm^{-1}).[19] All DNA molar concentrations reported herein are presented relative to base (which is equal to the number of phosphate groups). DMSO is known to induce denaturation of dsDNA.[20,21] However, we believe that this was not significant in our system in the presence of 4% (v/v) of DMSO, as studies on the effect of solvent composition on this process [with ca. (1−5) × 10^{-2} M electrolyte] showed that the midpoint of the denaturation transition corresponds to 62 vol % DMSO,[20] with no significant effect of salt concentration in the range between 10^{-3} and 5 × 10^{-2} M.[20] In agreement with this finding, experiments carried out with acridine orange, a dye sensitive to DNA secondary structure,[22] confirmed that DNA was not denatured in the presence of 4% DMSO (Supporting Information).

For conductivity experiments, dsDNA stock solutions of 3 × 10^{-3} M concentration were used. Various additions of this solution were made to a 4% DMSO−water HTMA-PFP solution (repeat unit concentration of 4.98 × 10^{-6} M). For viscosity measurements, various polymer−dsDNA and dsDNA solutions were prepared in 4% DMSO−water mixtures with DNA concentrations between 2 × 10^{-6} and 3 × 10^{-5} M and with an HTMA-PFP concentration of about 5.0 × 10^{-6} M (repeat units). A dsDNA stock solution 3.2 × 10^{-6} M, in Millipore-Q water, was used to obtain the appropriate DNA concentration. Freshly prepared solutions were used for viscosity measurements.

ssDNA stock solutions were prepared by heating dsDNA solutions at 85−90 °C for 15 min and dipping them immediately into ice for fast cooling to prevent renaturation.[23] From the decrease in light scattering observed in HTMA-PFP solutions upon addition of ssDNA compared to the changes in the scattering upon addition of dsDNA, we concluded that we had homogeneous solutions with no sign of any significant intramolecular interactions or microprecipitate formation as a result of DNA denaturalization.

Quinine sulfate from Fluka in 0.1 M sulfuric acid was used as the standard for quantum yield measurements.[24]

Apparatus and Methods. Absorption spectra were recorded on a Shimadzu 2501 PC UV−visible spectrophotometer. For steady-state luminescence spectral measurements, a Shimadzu RF-5301 PC instrument was used in a right-angle configuration. The excitation wavelength was 381 nm, and the excitation and emission slits were 3 and 1.5 nm, respectively. Both absorption and emission spectra were measured at 25.0 ± 0.1 °C. Polarized fluorescence spectroscopy experiments were also carried out. The fluorescence anisotropy of the sample was calculated according to the equation[25]

$$\langle r \rangle = \frac{I_{V,V} - GI_{V,H}}{I_{V,V} + 2GI_{V,H}} \quad (1)$$

where $I_{ex,em}$ is the intensity of the emission; V and H represent vertical and horizontal alignments, respectively, of the excitation and emission polarizers; and $G = I_{H,V}/I_{H,H}$ is the instrumental correction factor.

These experiments were carried out with a polarization setup consisting of two Glan−Thompson rotatable prism polarizers. The single-channel (L-format) method for fluorescence anisotropy determination was used. To calculate each anisotropy value via eq 1, four complete fluorescence spectra, one for every configuration of polarizers, were required. The fluorescence spectra for anisotropy experiments were recorded on a Jobin-Yvon Fluoromax-3 spectrometer with a right-angle geometry, exciting at 381 nm, with excitation and emission slits of 5 nm.

Time-resolved fluorescence measurements were carried out using a previously described single-photon-counting system with picosecond time resolution,[26] with an upgrade in the electronic detection system [an SPC-630 board module, from Becker & Hickl GmbH, replacing the constant fraction discriminators (CFDs), the time-to-amplitude converter (TAC), and the multichannel analyzer (MCA)]. Excitation of samples was carried out with the frequency-doubled output of an actively mode-locked picosecond Ti-sapphire laser (Spectra Physics Tsunami), pumped by a solid-state laser (Spectra Physics Millennia Xs). The repetition rate was 82 MHz. Excitation was vertically polarized, and emission was collected at a 90° geometry, passed through a polarizer at approximately 54.7° (Spindler & Hoyer Glan laser prism polarizer) and a monochromator (Jobin-Yvon H20 Vis) and detected with a microchannel plate photomultiplier tube (MCP-PT Hamamatsu R3809u-50). An inverted START−STOP configuration was used in the acquisition. The experimental instrumental response function was obtained for all excitation wavelengths [full width at half-maximum (fwhm) was 19 ps]. Alternate collection of the pulse profile and sample decays was performed (10^3 counts at the maximum per cycle) until between about 5 × 10^3 (typical) and 3 × 10^4 total detected counts had been accumulated at the maximum of the fluorescence signal. The fluorescence decays were deconvoluted using Striker et al.'s Sand program.[27]

Solution electrical resistances were measured using a Wayne-Kerr model 4265 Automatic LCR meter at 1 kHz. A Shedlovsky-type conductance cell was used.[28] The cell constant (0.0965 cm^{-1}) was determined to within ±0.02% from measurements with KCl (reagent-grade, recrystallized and dried using the procedure and data from Barthel et al.[29]). Measurements were made at 25.0 ± 0.1 °C with cells in a Selecta thermostat bath.

Dynamic viscosities, η, were measured with an automated AMV Anton Paar microviscometer. Viscosity measurements are based on the shear stress of a rolling ball introduced into an inclined, sample-filled glass capillary (1.6 mm in diameter) placed inside a thermostatted block (±0.01 °C) by measuring the time (±0.001 s) needed for the steel ball to roll a fixed distance between two sensors. The stress was varied by changing the inclination angle (60° and 70°). Viscosities were determined as an average of eight readings (two inclination angles, four readings each). Careful calibration was obtained at every inclination angle at 25 °C using water as the standard liquid and the density of the ball (7.630 g cm^{-3}).

Results and Discussion

The results are presented according to the techniques used: UV−visible absorption and stationary-state fluorescence, conductivity, viscosity, time-resolved fluorescence, and anisotropy.

UV−Visible Absorption and Stationary-State Fluorescence. In Figure 2, the variations of the absorption and emission spectra upon dsDNA additions are presented. The observed spectroscopic changes can be analyzed considering two different concentration ranges for both dsDNA and ssDNA: the first for DNA base concentrations up to that of the polymer repeat unit, and the second for higher concentrations.

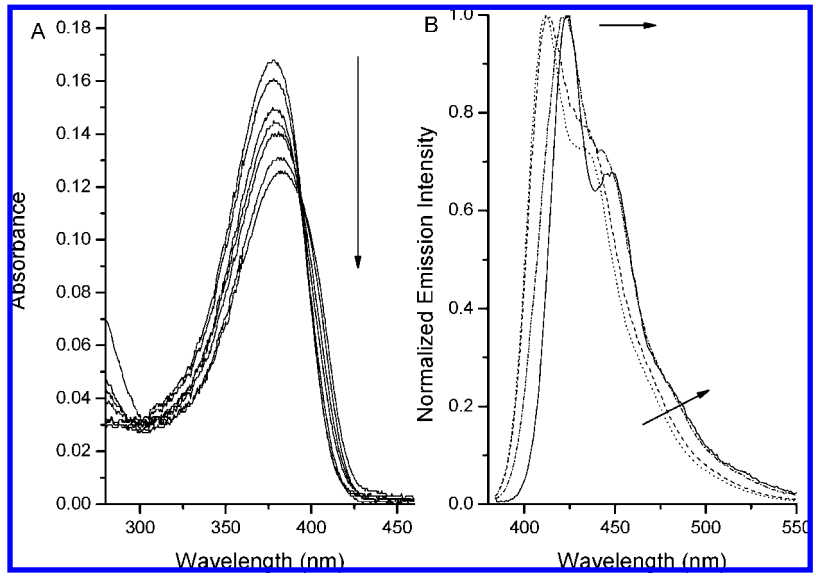

Figure 2. HTMA-PFP ($\overline{M_n}$ = 14.5 kg/mol, concentration = 3.35×10^{-6} M) in 4% DMSO−water mixtures with dsDNA additions: (A) absorption spectra ([DNA] = 0, 1.2×10^{-7}, 1.1×10^{-6}, 2.1×10^{-6}, 3.1×10^{-6}, 4.8×10^{-6}, and 9.6×10^{-6} M, relative to phosphate groups), (B) normalized emission spectra ([DNA] = 0, 2.1×10^{-6}, 4.7×10^{-6}, and 9.6×10^{-6} M in terms of base for dotted, dashed, dash-dotted, and solid lines, respectively).

Low DNA Concentrations. For DNA concentrations slightly lower than the concentration of polymer repeat units, a decrease in absorption and emission intensities was observed, with no significant changes in the spectral shapes (Figure 2A,B).

From the decrease of the maximum in the absorbance at 378 nm versus the molar ratio of DNA to HTMA-PFP (Figure 3A), we conclude that a 1:1 complex is formed between DNA and HTMA-PFP.

If we define ΔD as the difference in absorbance between free HTMA-PFP and HTMA-PFP in the presence of DNA (HTMA-PFP/DNA) at 378 nm (absorption wavelength maximum), the data can be fitted to the Benesi−Hildebrand equation (eq 2) for a 1:1 complex[30,31] (Figure 3B)

$$\Delta D = \frac{[\varepsilon_{\text{HTMA-PFP/DNA}} - \varepsilon_{\text{HTMA-PFP}}][\text{HTMA-PFP}]_0 K_A^{BH}[\text{DNA}]}{1 + K_A^{BH}[\text{DNA}]} \quad (2)$$

where $\varepsilon_{\text{HTMA-PFP/DNA}}$ and $\varepsilon_{\text{HTMA-PFP}}$ are the molar extinction coefficients of HTMA-PFP/DNA and free HTMA-PFP, respectively, at the titration wavelength; $[\text{HTMA-PFP}]_0$ is the initial HTMA-PFP concentration, and K_A^{BH} is the Benesi−Hildebrand association constant for complexes with 1:1 stoichiometry

$$\text{HTMA-PFP} + \text{DNA} \overset{K_A^{BH}}{\rightleftharpoons} \text{HTMA-PFP/DNA} \quad (3)$$

A good nonlinear fitting of ΔD versus DNA concentration was obtained (Figure 3B), in agreement with the equilibrium in eq 3. The calculated Benesi−Hildebrand constants are reported in Table 1. K_A^{BH} increases linearly with polymer molecular weight (Figure 3C) and is an order of magnitude higher for ssDNA than for dsDNA (Table 1). We believe that the stronger complexation between HTMA-PFP and ssDNA is favored by the higher flexibility of ssDNA, differences in charge density, and/or greater hydrophobicity, resulting from the bases being more exposed. This is consistent with studies on the effect of oppositely charged amphiphiles, which show a stronger interaction with ssDNA than dsDNA.[23,32,33] No significant changes either in the maximum absorbance variation with the DNA concentration (Figure 3) or in the calculated K_A^{BH} value (Table 1) were observed upon increasing the DNA molecular weight [dsDNA and dsDNA(HP)]. The Benesi−Hildebrand constant is slightly lower with dsDNA(HP). The increase in the Benesi−Hildebrand constant with conjugated polymer molecular weight might be associated with increased hydrophobic interactions.

The quenching of emission intensity follows Stern−Volmer kinetics for DNA concentrations lower than the concentration of polymer

$$\frac{F_o}{F} = 1 + K_{SV}[Q] \quad (4)$$

where F_o and F are the HTMA-PFP emission intensities in the absence and presence of quencher, respectively, and K_{SV} is the Stern−Volmer constant, which, for a purely dynamic process, can be expressed as $K_{SV} = \tau_0 k_q$. In this expression, τ_o is the polymer fluorescence lifetime in absence of DNA in 4% DMSO−water mixtures (0.52 ns), k_q is the quenching constant (in L s^{-1} mol^{-1}), and [Q] is the molar concentration of the quencher (in this case, DNA). The Stern−Volmer and quenching constants calculated for these systems (Table 2) are close to those obtained when sodium dodecyl sulfonate was added to the same polymer solution.[5b]

Although it is difficult to determine the diffusion-controlled rate constants in water in this system with oppositely charged species in the absence of the actual charge of HTMA-PFP, the fact that the apparent values of k_q are orders of magnitude higher than expected for pure water (a value $k_{diff} = 5.4 \times 10^{12}$ L s^{-1} mol^{-1} has been observed for reaction between a similar cationic conjugated polyelectrolyte and hydrated electrons)[34] strongly suggests a significant static component in the quenching. No clear correlation between the polymer molecular weight and the Stern−Volmer constants is observed, and ssDNA is apparently a more effective quencher than dsDNA. This is in agreement with the higher Benesi−Hildebrand association constants ob-

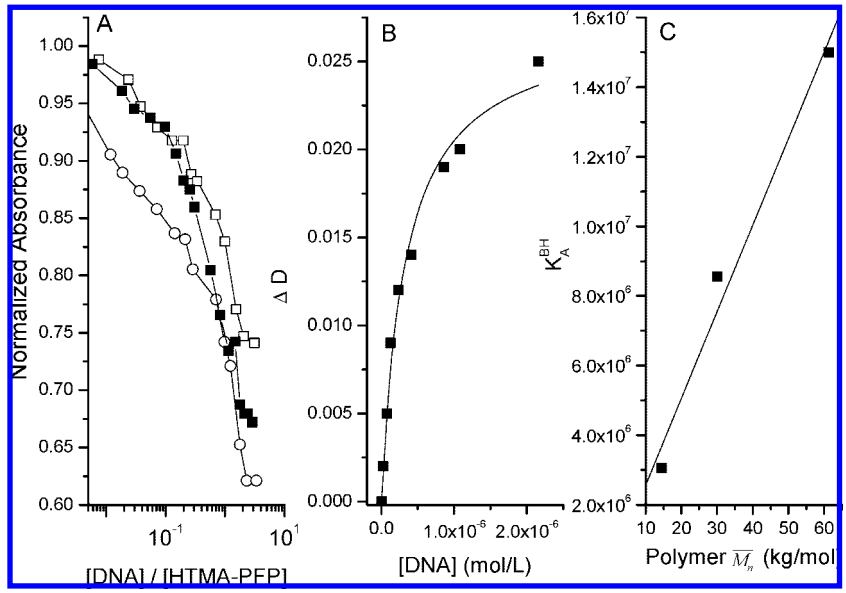

Figure 3. (A) HTMA-PFP ($\overline{M_n}$ = 14.5 kg/mol, concentration = 3.35 × 10^{-6} M, for experiments with salmon testes DNA; $\overline{M_n}$ = 30.1 kg/mol, concentration = 3.88 × 10^{-6} M, for experiments with human placenta DNA in 4% DMSO−water) normalized absorbance at the maximum of the spectra (378 nm) versus DNA-to-polymer concentration ratios (open squares, dsDNA; open circles, ssDNA; solid squares, dsDNA(HP) on a logarithmic scale. (B) Benesi−Hildebrand nonlinear plot (Δ*D* versus dsDNA molar concentration, eq 2, for dsDNA concentrations up to 3 × 10^{-6} M. (C) Benesi−Hildebrand association constants of the HTMA-PFP/dsDNA systems versus polymer molecular weight.

TABLE 1: Benesi−Hildebrand Association Constants (K_A^{BH})

$\overline{M_n}$ (kg/mol)	DNA	DNA concentration range (mol/L)	K_A ^{BH} (mol^{-1} L)
14.5	ds	0−2.1 × 10^{-6}	3.0 (±0.4) × 10^6
14.5	ss	0−7.8 × 10^{-7}	2.5 (±0.2) × 10^7
30.1	ds	0−7.8 × 10^{-7}	8.6 (±0.1) × 10^6
30.1	ds(HP)	0−4.6 × 10^{-7}	7.7 (±0.2) × 10^6
61.3	ds	0−7.4 × 10^{-7}	1.5 (±0.2) × 10^7

tained for association of HTMA-PFP with ssDNA (Table 1) and confirms the significant contribution of static quenching. The same conclusion can be reached when comparing the quenching (Table 2) and Benesi−Hildebrand association constants obtained with dsDNA(HP) and dsDNA (Table 1). The two constants are similar but slightly lower than those obtained with the higher-molecular-weight DNA (human placenta).

High DNA Concentrations (Higher Than the Polymer Concentration). For DNA concentrations above the polymer concentration, a more dramatic decrease of absorbance at 378 nm is seen, accompanied by a red shift (ca. 4 nm) and a broadening of the absorption spectrum.

The DNA concentration could be monitored through the changes in absorbance intensity because the dramatic decrease in absorbance finishes at DNA concentrations close to that of charge neutralization (where the concentration of DNA bases equal to twice the concentration of HTMA-PFP repeat units, because each monomer unit has two positive charges).

In addition, a well-defined isosbestic point appears at around 394 nm (Figure 2A). This could indicate that a new equilibrium is taking place, such as the formation of polymer aggregates between neutralized polymer chains as has been observed with the same polymer interacting with sodium *n*-alkyl sulfonate surfactants[5b]

$$P + P \overset{K_A}{\rightleftharpoons} A \tag{5}$$

Here, P represents the HTMA-PFP/DNA complex, A represents higher-order polymer aggregates formed as a consequence of the interaction between HTMA-PFP and DNA, and K_A is the aggregation constant. It has been well-established that the complexation of polyfluorenes with DNA or any other charged polyelectrolyte brings together polymer segments.[7g] It is also well-known that DNA condensation by proteins, polypeptides, or polycations leads in many cases to the formation of insoluble complexes and that aggregation between semirigid polyelectrolytes, such as DNA, and hairy-rod macromolecules in general can lead to complex macromolecular architectures.[35]

From a variation of an iterative method described initially to study aggregation of dyes in solution[36] and adapted to polymeric systems,[5b] the aggregate concentrations, aggregate absorption spectra, and K_A can be calculated for each DNA concentration.

The aggregation constant can be expressed as[36]

$$K_A = \frac{1 - x}{2cx^2} \tag{6}$$

where *x* is, in this case, the molar fraction of P and *c* is the polymer molar concentration.

The molar absorption coefficient at any wavelength ($\bar{\varepsilon}_\lambda$) can be expressed as

$$\bar{\varepsilon}_\lambda = \overline{\varepsilon_\lambda^P} x + \overline{\varepsilon_\lambda^A}(1 - x) \tag{7}$$

where $\overline{\varepsilon_\lambda^P}$ and $\overline{\varepsilon_\lambda^A}$ are the average molar absorption coefficients of P and A, respectively. It is assumed that P is the only species present for DNA concentrations of around 1 × 10^{-6} M (Table 2). Under these conditions, the absorption spectrum will be that of P: $\bar{\varepsilon}_\upsilon = \overline{\varepsilon_\lambda^P}$ (not very different from that of the free polymer in 4% DMSO−water, Figure 2)

From eq 7, the molar absorption coefficients of higher-order aggregates, $\overline{\varepsilon_\lambda^A}$, can be determined if *x* is known. The P molar fraction can be determined by an iterative method,[36] leading to a limiting *x* value obtained when differences of 0.004 are observed between consecutive calculated *x* values.

TABLE 2: Stern−Volmer (K_{SV}) and Quenching (k_q) Constants for HTMA-PFP (4% DMSO−Water) with DNA

$\overline{M_n}$ (kg/mol)	DNA	DNA concentration range (mol/L)	K_{SV} (L/mol)	k_q [L/(s mol)]
14.5	ds	$0-2.5 \times 10^{-6}$	$3.3\ (\pm 0.1) \times 10^5$	$6.4\ (\pm 0.2) \times 10^{14}$
14.5	ss	$0-3.0 \times 10^{-6}$	$6.6\ (\pm 0.4) \times 10^5$	$1.27\ (\pm 0.07) \times 10^{15}$
30	ds	$0-1.2 \times 10^{-6}$	$6.7\ (\pm 0.2) \times 10^5$	$1.29\ (\pm 0.05) \times 10^{15}$
30.1	ds(HP)	$0-1.2 \times 10^{-6}$	$3.7\ (\pm 0.1) \times 10^5$	$7.09\ (\pm 0.06) \times 10^{14}$
61.3	ds	$0-2.1 \times 10^{-6}$	$2.5\ (\pm 0.4) \times 10^5$	$4.8\ (\pm 0.5) \times 10^{14}$

TABLE 3: Aggregation Constants for Species Produced by Charge Neutralization of HTMA-PFP by DNA

$\overline{M_n}$ (kg/mol)	DNA	DNA concentration range (mol/L)	K_A (mol^{-1} L)
14.5	ds	$2.1-4.7 \times 10^{-6}$	$2.7\ (\pm 1.6) \times 10^5$
14.5	ss	$3.1-29 \times 10^{-6}$	$2.2\ (\pm 0.9) \times 10^5$
30.1	ds	$3.1-15 \times 10^{-6}$	$1.4\ (\pm 0.4) \times 10^5$
30.1	ds(HP)	$9.3-21 \times 10^{-6}$	$3.1\ (\pm 0.6) \times 10^5$
61.3	ds	$9.0-75 \times 10^{-6}$	$2.9\ (\pm 0.8) \times 10^5$

The parameter R is defined as[36]

$$R = \frac{A_{\lambda A}}{A_{\lambda P}} = \frac{\overline{\varepsilon^{P}_{\lambda A}} x + \overline{\varepsilon^{A}_{\lambda A}}(1-x)}{\overline{\varepsilon^{P}_{\lambda P}} x + \overline{\varepsilon^{A}_{\lambda P}}(1-x)} \quad (8)$$

where $A_{\lambda P}$ and $A_{\lambda A}$ are the experimental absorbances of P and A, respectively, at their wavelength maxima. The maximum absorbance wavelength of P is assumed to be that of the HTMA-PFP absorption spectrum with DNA concentrations of around 1×10^{-6} M (around 378 nm). The absorption maximum for A (405 nm) was calculated by subtracting the absorption spectrum of the sample with a DNA concentration of 1×10^{-6} M from the HTMA-PFP absorption spectrum at the highest DNA concentration used in this study for every system (between 1×10^{-5} and 7×10^{-5} M).

Parameter R becomes R_o when $x \approx 1$[36] (i.e., for a DNA concentration 1×10^{-6} M)

$$R_0 = \frac{\overline{\varepsilon^{P}_{\lambda A}}}{\overline{\varepsilon^{P}_{\lambda P}}} \quad (9)$$

To obtain a first approximate value of $x^{(1)}$, it is assumed that $\overline{\varepsilon^{A}_{\lambda P}} \ll \overline{\varepsilon^{P}_{\lambda P}}$ and $\overline{\varepsilon^{A}_{\lambda A}} \approx \overline{\varepsilon^{P}_{\lambda A}}$, leading to an approximate molar fraction that allows for the calculation of K_A, the molar concentration of A, $\overline{\varepsilon^{A}_{\lambda A}}$, and $\overline{\varepsilon^{A}_{\lambda P}}$ from eqs 6 and 7

$$x^{(1)} = \frac{R_0}{R} \quad (10)$$

These calculated average molar absorption coefficient values were then used to estimate a second value of x with eq 8, as well as a second value of association constant and aggregate molar absorption coefficients (eqs 6 and 7). The convergence of the x values was normally reached with less than 10 iterations. With these x values, the aggregate absorption spectra were calculated from eq 7.

The average aggregation constants for each system are reported in Table 3, and the absorption spectra of the aggregate exhibited a maximum around 400 nm (Figure 4). These spectra are close to but slightly blue-shifted from those obtained for HTMA-PFP aggregates induced upon charge neutralization with *n*-alkyl sulfonate surfactants (absorption maximum at 402 nm).[5b] This small spectral shift could be attributed to environmental effects or some differences in the kind of aggregates formed. The aggregation constants are of the same order of magnitude as those for aggregates of HTMA-PFP ($\overline{M_n} = 14.5$ kg/mol) with alkyl sulfonates [$(4 \times 10^5)-(1 \times 10^6)$ mol^{-1} L].[5b]

No significant differences were observed with the HTMA-PFP molecular weight or with the DNA secondary structure and molecular weight (salmon testes and human placenta DNA).

We also monitored the effect of DNA concentration through changes in both the fluorescence emission spectral shape and the quantum yield. Changes in the vibrational structure of the emission spectra provide further spectral evidence of DNA interactions (Figure 5A). For DNA concentrations between those of the polymer repeat units and charge neutralization, the ratio of the intensities of the main emission maximum and the first shoulder ($I_{max}/I_{shoulder}$ taken at 412 and 434 nm) decreases and reaches its lowest value when the charges are neutralized (Figure 5A). The maximum is significantly shifted (11−12 nm) to the red when the DNA concentration equals that of the polymer repeat units (Figure 5B). Moreover, within the same DNA concentration range, a dramatic decrease in emission quantum yield is observed (Figure 5C). This does not follow Stern−Volmer kinetics and can be attributed to the formation of polymer aggregates, as previously indicated from absorption spectral data. ϕ reaches a minimum when the DNA concentration corresponds to charge neutralization. From these results, we see that the maximum emission shifts, spectrum shape, and emission quantum yield of HTMA-PFP in the presence of DNA can all be used to determine the DNA concentration in solution. No significant differences were observed between dsDNA and ssDNA or for different DNA molecular weights (Figure 5).

Our results are in perfect agreement with a Monte Carlo simulation on the formation of complexes in solutions containing polycations and variable amounts of polyanions in the absence of added salt carried out by Hayashi et al.[37] using a simple spring−bead model. Systems that contain 10 polycations and 5

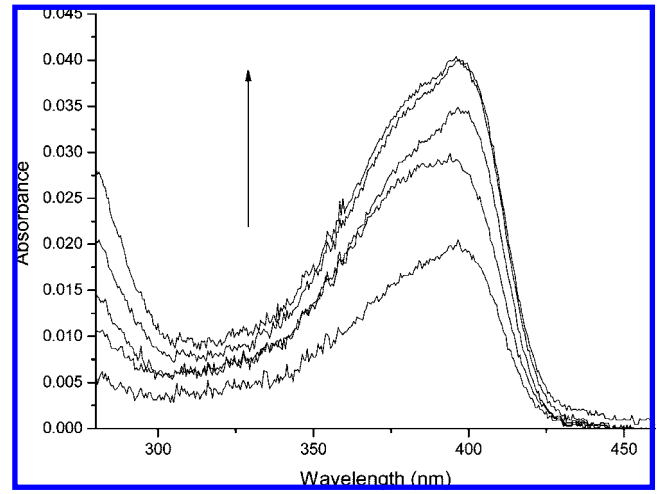

Figure 4. HTMA-PFP ($\overline{M_n}$ =14.5 kg/mol, 3.35×10^{-6} M) aggregate absorbance spectra for DNA concentrations of 3×10^{-6}, 4.7×10^{-6}, 6.3×10^{-6}, and 9.6×10^{-6} M.

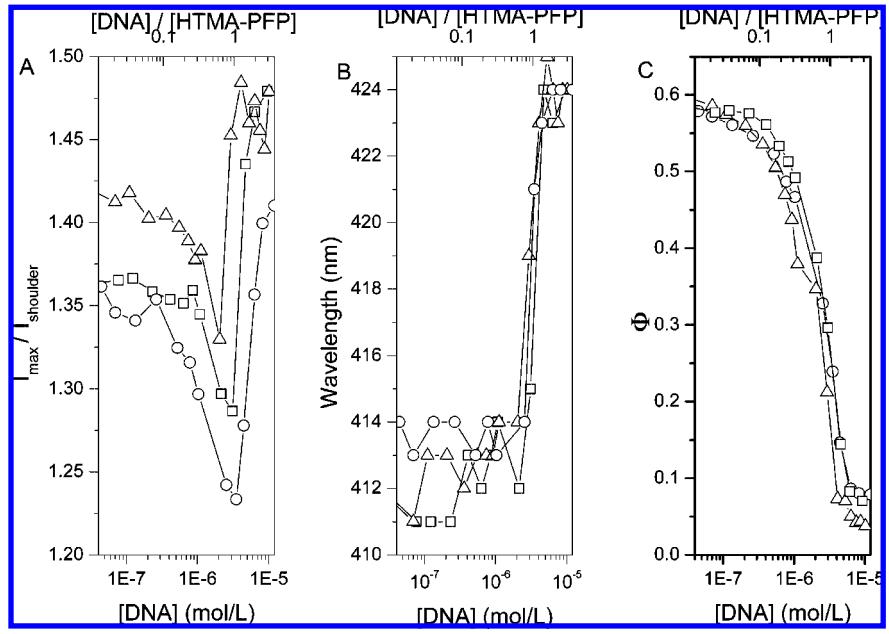

Figure 5. HTMA-PFP ($\overline{M_n}$ = 14.5 kg/mol, concentration = 3.35×10^{-6} M, for experiments with salmon testes DNA; $\overline{M_n}$ = 30.1 kg/mol, concentration = 3.88×10^{-6} M, for experiments with human placenta DNA in 4% DMSO−water): (A) emission intensity ratio ($I_{max}/I_{shoulder}$ of the emission spectra) versus DNA concentration on a logarithmic scale, (B) emission maximum wavelength versus DNA concentration on a logarithmic scale, (C) emission quantum yield variation versus DNA concentration on a logarithmic scale. Squares, dsDNA; circles, ssDNA; triangles, dsDNA(HP).

polyanions with the same absolute charge are dominated by 2:1 clusters, kept apart by a net repulsion. When equal amounts of polyions are present, neutral clusters of small to intermediate sizes dominate the system. However, if the polycations and polyanions have unequal lengths (as in our case), the propensity for forming larger clusters increases considerably in systems with equal amounts of positive and negative polyion charges. Although the model is simple compared to our systems, there is a fairly good agreement given that we observe the formation of clusters upon charge neutralization and, below that point, our 1:1 complex (polymer/DNA, in repeat units and phosphate groups, respectively) corresponds in terms of charges to the 2:1 cluster (polycation/polyanion) of the theoretical study because every polymer repeat unit has twice the charge of a DNA phosphate group.

Conductivity. The electrical specific conductance, κ, of HTMA-PFP ($\overline{M_n}$ = 30.1 and 61.3 kg/mol) in DMSO−water mixtures (4% v/v) was measured, as a function of dsDNA concentration. Five blanks were also recorded by measuring the κ values of dsDNA solutions with the same concentration in this solvent mixture. The experimental κ data were corrected by subtracting the κ value of the solvent (4% DMSO−water, v/v) in the case of the blanks and the κ values of the polymer solution in the absence of DNA for the experiments carried out in the presence of polymer. Hereafter, we indicate the corrected data by κ'. In both cases, dsDNA additions induce nonlinear increases in κ' (inset of Figure S2 of the Supporting Information).

As was seen with the spectroscopic results, the largest difference between the HTMA-PFP/dsDNA systems and the blank ($\Delta\kappa' = \kappa'_{\text{HTMA-PFP/dsDNA}} - \kappa'_{\text{dsDNA}}$) occurs for dsDNA concentrations between the regions of 1:1 complexation and charge neutralization (between 5.5×10^{-6} and 1.1×10^{-5} M; Figure S2, Supporting Information). In this range, dsDNA additions increase the specific conductance less in the presence of the polymer than in the blank experiment, providing experimental evidence of electrostatic interactions between the polymer and dsDNA and showing that HTMA-PFP can be used as a conductivity probe to determine the DNA concentration in solution.

For dsDNA concentrations outside this region, the slopes for the variation of κ' with dsDNA concentration are similar for blank and polymer/dsDNA systems. At very low DNA concentrations, this effect could be due to the compensation of two opposing phenomena: the increase due to the release of polymer counterions on the interaction with DNA and the decrease of κ' as a consequence of the interaction between these two oppositely charged polyelectrolytes (HTMA-PFP and DNA). No significant effects of the polymer molecular weight on the conductivity behavior were observed.

Viscosity. The above results all demonstrate the dramatic effect on physical properties of HTMA-PFP charge neutralization upon the addition of dsDNA. Another relevant physicochemical property is the viscosity of the solution, as shown in Figure 6, for the intermediate- and highest-molecular-weight polymers. When dsDNA is added to a DMSO−water mixture (4% v/v), the viscosity of the solution increases linearly. However, in the presence of HTMA-PFP, the viscosity is constant until the polymer neutralization point is reached. Above this point, a strong increase is observed, strongly supporting the formation of polymer/DNA complexes.

The viscosity variation above polymer charge neutralization is more dramatic in the presence of HTMA-PFP than with dsDNA in the absence of the polymer. This strongly supports the conclusion of induced polymer aggregation by dsDNA polymer charge neutralization and the growth of mixed polymer aggregates.

Time-Resolved Fluorescence Studies. Fluorescence decays of the HTMA-PFP ($\overline{M_n}$ = 14.5 kg/mol)/dsDNA system were measured at different DNA concentrations. Emission was recorded at 416 and 450 nm (maximum and shoulder region), with excitation at 380 nm. No significant differences were observed between the sets of data obtained at the two wavelengths. Good global fits of the fluorescence decays measured

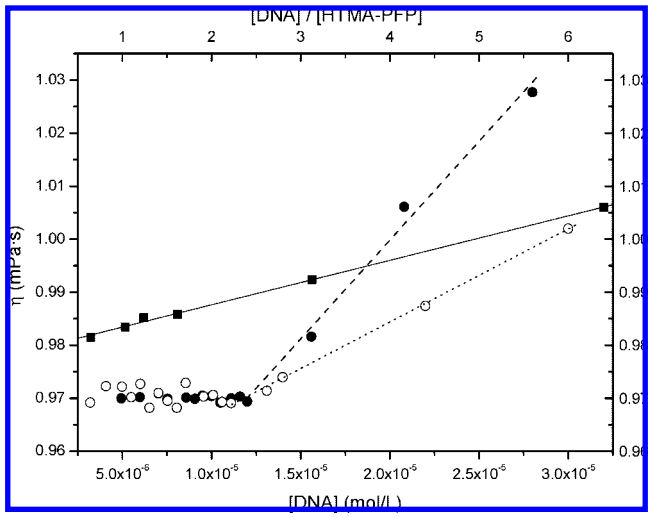

Figure 6. Dynamic viscosity of solutions of dsDNA in 4% DMSO−water mixtures alone (solid squares, solid line) and in the presence of HTMA-PFP (solid circles and dashed line, $\overline{M_n} = 30.1$ kg/mol and concentration $= 5.00 \times 10^{-6}$ M; open circles and dotted line, $\overline{M_n} = 61.3$ kg/mol and concentration $= 4.98 \times 10^{-6}$ M).

at the two emission wavelengths were obtained with sums of three exponential terms (Table S1 in the Supporting Information).

In the absence of DNA, the decay times were 483, 78.4, and 8.9 ps. The longest decay time is assigned to the pure polymer, because it is the main component in the solution and because its value is similar in magnitude to the lifetimes of other polyfluorenes: 360 ps for PBS-PFP[38] and 340 ps for poly(9,9-dioctylfluorene) in MCH at 298 K.[39]

From the decay times, τ_i, and the respective pre-exponential factors a_i (Table S1 in the Supporting Information), the relative contributions of the three decay components to the total time-integrated fluorescence ($I_i = \int_0^\infty a_i e^{-t/\tau_i}\, dt = a_i\tau_i$) can be calculated. The variation of the percentage of the fluorescence contribution of the longest decay time, I_1, upon dsDNA addition is similar to that of the steady-state emission intensity, whereas the sum of amplitudes of the two shortest-lived species ($I_2 + I_3$) behaves in the opposite way (Figure S3 in the Supporting Information). This trend is much more closely related to the pre-exponential factor than to the decay time itself, and it seems that the long-lived component is replaced by the short-decay-time species. This is similar to what was previously observed upon interaction of HMTA-PFP with *n*-decyl sulfonates.[5b] As was discussed in that case,[5b] the two short-lived components are likely to be due to the polymer aggregates formed upon neutralization of polymer charge, which is by DNA in the present case, in agreement with the absorption spectral results.

Fluorescence Anisotropy. The fluorescence anisotropy ($\langle r \rangle$, eq 1) of HTMA-PFP ($\overline{M_n} = 14.5$, 30.1, and 61.3 kg/mol) was measured in DMSO−water (4%, v/v) solutions with polymer concentrations of 3.58, 4.20, and 7.2 μM (in terms of repeat units) and various dsDNA additions. Upon addition of dsDNA, the anisotropy decreases (Figure S4 in the Supporting Information), reaching a minimum between the regions of 1:1 complexation and charge neutralization, providing further evidence of the interaction between the polymer and dsDNA. The decrease of the anisotropy with DNA concentration is more pronounced for the lower-molecular-weight polymer, which also shows the higher anisotropy value.

The loss in fluorescence anisotropy in HTMA-PFP can be attributed to three different mechanisms: rotational diffusion,[25] exciton migration, and conformational relaxation (twisting of part of the aromatic backbone).[40] Attempts were made to correlate the changes of anisotropy with lifetime measurements to obtain rotational diffusion coefficients[25] and relate the variation of these constants through a modified Stokes−Einstein equation with the viscosity of the solutions. However, the results obtained were physically meaningless (i.e., diffusion coefficients were seen to increase with viscosity), which rules out diffusion as the main factor to explain the anisotropy variations in these systems. Further, we also believe that, if conformational relaxation were the dominant mechanism, there would be no obvious reason with these systems (where the contour length of the polymers is significantly greater than the conjugation length) for the anisotropy results to depend on the polymer molecular weight. We therefore conclude that intermolecular excitation migration, favored by polymer aggregation, is probably the key factor to explain the changes in anisotropy. We have previously shown that energy migration in an anionic polyfluorene is favored by the increase of polymer interchain interaction induced by charge neutralization by oppositely charged surfactants.[5a]

Conclusions

Two distinct processes are observed in the interaction between DNA and the cationic polyfluorene HTMA-PFP in aqueous solutions. For DNA concentrations (in terms of bases or phosphate groups) below the concentration of the polymer (in repeat units), a 1:1 HTMA-PFP/DNA complex is formed, whose association constant can be calculated from changes in the absorption spectra using the Benesi−Hildebrand equation. The values are higher for ssDNA than for dsDNA, probably as a consequence of greater flexibility, differences in charge density, and a more hydrophobic character. This constant also increases linearly with polymer molecular weight, possibly as a result of increased hydrophobic interactions. For higher DNA concentrations, in the region of charge neutralization, polymer aggregation is observed. The aggregate absorption spectra and formation constants can be calculated from changes in the absorption spectra. Aggregation is more marked with dsDNA, possibly as a result of decreased charge screening in comparison with ssDNA.

The point of electroneutrality can be determined from absorption or emission spectra, changes in electrical conductivity, and changes in viscosity, providing routes that can be used for the determination of DNA concentration in solution.

The most sensitive techniques are the spectroscopic ones, with changes between 35% and 80% in the case of absorbance and emission intensity, respectively, upon polymer charge neutralization with DNA, and the conductivity, with changes of about 50% at electroneutrality. Although viscosity is much less sensitive, with changes of about 4% at electroneutrality, it supports the overall picture of polymer/DNA interactions indicated from the other methods.

Moreover, the minimum amount of DNA that can be detected is conditioned by the minimum amount of polymer necessary to obtain good spectroscopic signals or induce sufficient changes in conductivity and viscosity compared to those of the pure solvent and is around micromolar.

Time-resolved fluorescence experiments show that the fluorescence decays can be fitted to three exponentials, with the two short-lived components attributed to the polymer aggregates. Evidence for HTMA-PFP/DNA aggregation also comes from the decrease in polymer fluorescence anisotropy with DNA

concentration, which is suggested to be mainly due to exciton migration favored by interchain interaction in the polymer aggregates.

The aggregates produced upon charge neutralization could provide interesting macromolecular architectures for various applications. Future experiments will be designed to attempt to clarify their structures.

Acknowledgment. MEC and FEDER are thanked for financial support through Project MAT2004-03827 and POCI/FCT/FEDER through Project POCI/QUI/58291/2004. M.J.T. thanks Burgos University for financial support during a short stay at Coimbra University. R.E.D.P. thanks FCT for a postdoctoral grant (BPD/34558/2007).

Supporting Information Available: Details on studies of the denaturation of DNA in DMSO−water mixtures, conductivity, time-resolved fluorescence, and fluorescence anisotropy. This material is available free of charge via the Internet at http://pubs.acs.org.

References and Notes

(1) Pinto, M. R.; Schanze, K. S. *Synthesis* **2002**, *9*, 1293–1309.

(2) (a) Burrows, H. D.; Fonseca, S. M.; Silva, C. L.; Pais, A. A. C. C.; Tapia, M. J.; Pradhan, S.; Scherf, U. *Phys. Chem. Chem. Phys.* **2008**, *10*, 4420–4428. (b) Gaylord, B. S.; Wang, S. J.; Heeger, A. J.; Bazan, G. C. *J. Am. Chem. Soc.* **2001**, *123*, 6417–6418. (c) Lee, K.; Povlich, L. K.; Kim, J. *Adv. Funct. Mater.* **2007**, *17*, 2580–2587.

(3) (a) Yang, R.; Wu, H.; Cao, Y.; Bazan, G. C. *J. Am. Chem. Soc.* **2006**, *128*, 14422–14423. (b) Shi, W.; Fan, S.; Huang, F.; Yang, W.; Liu, R.; Cao, Y. *J. Mater. Chem.* **2006**, *16*, 2387–2394. (c) Morgado, J.; Barbagallo, N.; Charas, A.; Alcácer, L. *Synth. Met.* **2004**, *141*, 219–223. (d) Neher, D.; Grüner, J.; Cimrová, V.; Schmidt, W.; Rulkens, R.; Lauter, U. *Polym. Adv. Techol.* **1998**, *9*, 461–475.

(4) (a) Zhang, Y.; Liu, B.; Cao, Y. *Chem. Asian J.* **2008**, *3*, 739–745. (b) Herland, A.; Inganäs, O. *Macromol. Rapid Commun.* **2007**, *28*, 1703–1713. (c) Peng, H.; Soeller, C.; Travas-Sejdic, J. *Chem. Commun.* **2006**, 3735–3737. (d) Huang, F.; Wang, X.; Wang, D.; Yang, W.; Cao, Y. *Polymer* **2005**, *46*, 12010–12015. (e) Achyuthan, K. E.; Bergstedt, T. S.; Chen, L.; Jones, R. M.; Kumaraswamy, S.; Kushon, S. A.; Ley, K. D.; Lu, L.; McBranch, D.; Mukundan, H.; Rininsland, F.; Shi, X.; Xia, W.; Whitten, D. G. *J. Mater. Chem.* **2005**, *15*, 2648–2656. (f) Chen, L.; McBranch, D. W.; Wang, H. L.; Helgeson, R.; Wudl, F.; Whitten, D. G. *Proc. Natl. Acad. Sci. U.S.A.* **1999**, *96*, 12287–12292.

(5) (a) Tapia, M. J.; Burrows, H. D.; Valente, A. J. M.; Pradhan, S.; Scherf, U.; Lobo, V. M. M.; Pina, J.; Seixas de Melo, J. *J. Phys. Chem. B* **2005**, *109*, 19108–19115. (b) Monteserín, M.; Burrows, H. D.; Valente, A. J. M.; Lobo, V. M. M.; Mallavia, R.; Tapia, M. J.; García-Zubiri, I. X.; Di Paolo, R. E.; Maçanita, A. L. *J. Phys. Chem. B* **2007**, *111*, 13560–13569.

(6) (a) Ho, H. A.; Dore, K.; Boissinot, M.; Bergeron, M. G.; Tanguay, R. M.; Boudreau, D.; Leclerc, M. *J. Am. Chem. Soc.* **2005**, *127*, 12673–12676. (b) Karlsson, K. F.; Aasberg, P.; Nilsson, K. P. R.; Inganaes, O. *Chem. Mater.* **2005**, *17*, 4204–4211. (c) Ho, H.-A.; Boissinot, M.; Bergeron, M. G.; Corbeil, G.; Dore, K.; Boudreau, D.; Leclerc, M. *Angew. Chem., Int. Ed.* **2002**, *41*, 1548–1551.

(7) (a) Baker, E. S.; Hong, J. W.; Gaylord, B. S.; Bazan, G. C.; Bowers, M. T. *J. Am. Chem. Soc.* **2006**, *128*, 8484–8492. (b) Liu, B.; Bazan, G. C. *Macromol. Rapid Commun.* **2007**, *28*, 1804–1808. (c) Woo, H. Y.; Vak, D.; Korystov, D.; Mikhailovsky, A.; Bazan, G. C.; Kim, D.-Y. *Adv. Funct. Mater.* **2007**, *17*, 290–295. (d) Liu, B.; Bazan, G. C. *Chem. Asian J.* **2007**, *2*, 499–504. (e) Hong, J. W.; Hemme, W. L.; Keller, G. E.; Rinke, M. T.; Bazan, G. C. *Adv. Mater.* **2006**, *18*, 878–882. (f) Liu, B.; Bazan, G. C. *Chem. Mater.* **2004**, *16*, 4467–4476. (g) Liu, B.; Bazan, G. C. *J. Am. Chem. Soc.* **2004**, *126*, 1942–1943. (h) Gaylord, B. S.; Heeger, A. J.; Bazan, G. C. *J. Am. Chem. Soc.* **2003**, *125*, 896–900. (i) Xu, Q.-H.; Gaylord, B. S.; Wang, S.; Bazan, G. C.; Moses, D.; Heeger, A. J. *Proc. Natl. Aca. Sci. U.S.A.* **2004**, *101*, 11634–11639. (j) Pu, K.-Y.; Pan, S. Y.-H.; Liu, B. *J. Phys. Chem. B* **2008**, *112*, 9295–9300.

(8) Bazan, G. C. *J. Org. Chem.* **2007**, *72*, 8615–8635.

(9) Gaylord, B. S.; Massie, M. R.; Feinstein, S. C.; Bazan, G. C. *Proc. Natl. Acad. Sci. U.S.A.* **2005**, *102*, 34–39.

(10) Liu, B.; Bazan, G. C. *Chem. Asian J.* **2007**, *2*, 499–504.

(11) Chi, C.; Mikhailovsky, A.; Bazan, G. C. *J. Am. Chem. Soc.* **2007**, *129*, 11134–11145.

(12) Gaylord, B. S.; Heeger, A. J.; Bazan, G. C. *Proc. Natl. Acad. Sci. U.S.A.* **2002**, *99*, 10954–10957.

(13) Wang, S.; Bazan, G. C. *Chem. Commun.* **2004**, 2508–2509.

(14) (a) Al Attar, H. A.; Norden, J.; O'Brien, S.; Monkman, A. P. *Biosens. Bioelectron.* **2008**, *23*, 1466–1472. (b) Al Attar, H. A.; Monkman, A. P. *J. Phys. Chem. B* **2007**, *111*, 12418–12426.

(15) Mallavia, R.; Montilla, F.; Pastor, I.; Velásquez, P.; Arredondo, B.; Álvarez, A. L.; Mateo, C. R. *Macromolecules* **2005**, *38*, 3185–3192.

(16) Molina, R. Ph.D. Thesis, University Miguel Hernandez, Alicante, Spain, 2007.

(17) Mallavia, R.; Martinez-Peréz, D.; Chmelka, B. F.; Bazan, G. C. *Bol. Soc. Esp. Ceram. V* **2004**, *43*, 327–330.

(18) Liu, B.; Gaylord, B. S.; Wang, S.; Bazan, G. C. *J. Am. Chem. Soc.* **2003**, *125*, 6705–6714.

(19) Costa, D.; Burrows, H. D.; da Graça Miguel, M. *Langmuir* **2005**, *21*, 10492–10496.

(20) Herskovits, T. T. *Arch. Biochem. Biophys.* **1962**, *97*, 474–484.

(21) Seto, D. *Nucleic Acids Res.* **1990**, *18*, 5905–5906.

(22) Ichimura, S.; Zama, M.; Fujita, H. *Biochem. Biophys. Acta* **1971**, *240*, 485–495.

(23) Rosa, M.; Dias, R.; da Graça Miguel, M.; Lindman, B. *Biomacromolecules* **2005**, *6*, 2164–2171.

(24) Demas, J. N.; Crosby, G. A. *J. Phys. Chem.* **1971**, *75*, 991–1024.

(25) Lakowicz, J. R. In *Principles of Fluorescence Spectroscopy*, 1st ed.; Plenum Press, New York, 1983.

(26) Giestas, L.; Yihwa, C.; Lima, J. C.; Vantier-Giongo, C.; Lopes, A.; Maçanita, A. L.; Quina, F H. *J. Phys. Chem. A* **2003**, *107*, 3263–3269.

(27) Striker, G.; Subramaniam, V.; Seidel, C. A. M.; Volkmer, A.; J, *J. Phys. Chem. B* **1999**, *103*, 8612–8617.

(28) Vink, H. *J. Chem. Soc., Faraday Trans. I* **1981**, *77*, 2439–2449.

(29) Barthel, J.; Feuerlein, F.; Neuder, R.; Wachter, R. *J. Sol. Chem.* **1980**, *9*, 209–219.

(30) Benesi, H. A.; Hildebrand, J. H. *J. Am. Chem. Soc.* **1949**, *71*, 2703–2707.

(31) Balón, M.; Muñoz, M. A.; Carmona, C.; Guradado, P.; Galán, M. *Biophys. Chem.* **1999**, *80*, 41–52.

(32) Dias, R. S.; Lindman, B. *DNA interactions with Polymers and Surfactants*; John Wiley & Sons, Inc: New York, 2008.

(33) Morán, M. C.; Miguel, M. G.; Lindman, B. *Langmuir* **2007**, *23*, 6478–6481.

(34) Arnaut, L.; Formosinho, S.; Burrows, H. In *Chemical Kinetics: From Molecular Structure to Chemical Reactivity*; Elsevier: Amsterdam, 2007.

(35) (a) Wegner, G. *Macromol. Chem. Phys.* **2003**, *204*, 347–357. (b) Limbach, H. J.; Holm, C.; Kremer, K. *Macromol. Chem. Phys.* **2005**, *206*, 77–82.

(36) López Arbeloa, I. *J. Chem. Soc., Faraday Trans. 2* **1981**, *77*, 1725–1733.

(37) Hayashi, Y.; Ullner, M.; Linse, P. *J. Phys. Chem. B* **2003**, *107*, 8198–8207.

(38) Burrows, H. D.; Lobo, V. M. M.; Pina, J.; Ramos, M. L.; Seixas de Melo, J.; Valente, A. J. M.; Tapia, M. J.; Pradhan, S.; Scherf, U. *Macromolecules* **2004**, *37*, 7425–7427.

(39) Dias, F. B.; Morgado, J.; Maçanita, A. L.; da Costa, F. P.; Burrows, H. D.; Monkman, A. P. *Macromolecules* **2006**, *39*, 5854–5864.

(40) Vaughan, H. L.; Dias, F. M. B.; Monkman, A. P. *J. Chem. Phys.* **2005**, *122*, 014902.

JP806353Y